E-ISSN : 2541-5794
P-ISSN : 2503-216X

Journal of Geoscience,
Engineering, Environment, and Technology
Vol xx No xx 20xx

RESEARCH ARTICLE

Mineralogical and Geochemical Clay Analysis for Portland Cement Quality Distribution: A Study Case From Ajibarang District, Central Java, Indonesia

Izdihar Sahda Abidin [1] , Siswandi [1], Akhmad Khahlil Gibran [1]*

[1] *Geological Engineering, Faculty of Engineerring, Jederal Soedirman University, Mayjen Sungkono Street, 5 KM, Kalimanah, Purbalingga, Indonesia*

* Corresponding author : akgibran@unsoed.ac.id
Tel.:+62-851-7501-9633; fax: (0281) 6596700
Received: Oct 1, 2016; Accepted: Nov 20, 2016.
DOI: 10.24273/jgeet.2016.1.2.001

Abstract

Nowadays, the development of infrastructure has caused an increase in the need for cement. To determine the suitability of the raw materials used in cement production, an assessment must be carried out on the quality anMineralogical and Geochemical Clay Analysis for Portland Cement Quality Distribution: A Study Case From Ajibarang District, Central Java, Indonesiad suitability of the cement raw materials. This research was conducted in Halang Formation of the Tipar Kidul area and around Banyumas Regency, Central Java. The methods used are X-ray fluorescence (XRF) and scanning electron microscopy (SEM). Data from XRF analysis generally shows SiO_2 values from 26.83% to 57.75%, Al_2O_3 values from 11.18% to 20.23%, and Fe_2O_3 values from 3.21% to 8.76%. Judging from the aluminum index (AI) content, the ideal cement raw materials are two samples with a proportion of 3.17% to 3.22%. The results of SEM analysis show that there are illite, calcite, quartz and smectite minerals in the claystone research area. Based on data, almost 75% of the claystone survey area was found to be suitable as a raw material for cement. This research has a positive impact on the characterization of limestone as a raw material for cement by utilizing geochemical analysis and electron microscopy to achieve a more comprehensive understanding of the evaluation of limestone quality.

Keywords: Claystone XRF, SEM, Cement.

1. Introduction

The rapid expansion of infrastructure in Indonesia has increased the need for construction raw materials, especially cement (Marin et al., 2022). Claystone is one of the main raw materials for cement, along with limestone, which is made from hydrated aluminum silicate (Pettijohn, 1975). Evaluating the quality and suitability of clay is crucial as it plays a significant role in the formation of clinker within the cement industry.

In analyzing the quality of claystone as a raw material for cement, it is necessary to correlate the type of claystone mineral and the compound content in the claystone to determine which claystone is the best as a raw material for cement. Claystone quality control can be determined by analyzing its compounds using the X-ray fluorescence (XRF) technique (Gifford et al., 2020; Goldstein et al., 2018) and the mineral content of claystone can be determined using the scanning electron microscopy (SEM) analysis method (A. Gibran et al., 2022). The research was conducted in the mining area of PT. Sinar Tambang Arthalestari, Tipar Kidul, and its surroundings, Banyumas Regency, Central Java.

2. Literature Review

Claystone is a rock composed of hydrated aluminum silicate and is classified as a fine-grained sedimentary rock with the general formula $2H_2OAL_2O_32SiO_2$, where H_2O = water, Al = aluminum ion, O = oxygen, and SiO_2 = silicate (Welton, 2020).

Based on the classification of the suitability of claystone quality as a cement raw material according to (PT. Sinar Tambang Arthalestari, 2023) cement raw material standards. The maximum percentage of Al_2O_3 composition at Sinar Tambang Arthalestasi is 25%, the minimum percentage of SiO_2 is 52%, and the maximum percentage of Fe_2O_3 is 15%. The alumina index ranges from 3.16% to 3.44%.

According to Wilkins (2014), claystones can be grouped based on the relative size and thickness of clay minerals in general. This type of clay mineral consists of montmorillonite, which is 3 nm thick and 100 nm to 1000 nm in diameter (Welton, 2020). Illite and chlorite are 30 nm thick and 10,000 nm in diameter. Kaolinite is thicker than 50 nm to 2000 nm and has a diameter of 300 nm to 4000 nm (Welton, 2020).

3. Metodology

Two analyses were used when conducting claystone quality studies in the study area. We carried out geochemical analysis with X-ray fluorescence (XRF) (Gifford et al., 2020) and mineral type analysis with scanning electron microscopy (SEM) (Gibran et al., 2020). In carrying out the analysis, 18 samples were used for geochemical analysis and 3 samples for the analysis of claystone mineral types.

We carried out the sampling using the grab sampling method. Grab sampling is a random sampling method that involves taking parts of a material without special selection. Sampling uses this method to obtain samples that represent the specific quality conditions of the sample at the time of collection. Sampling is synchronized with the laws of stratigraphy, namely representing rock areas from oldest to youngest rocks.

The geochemical analysis is related to the standard content of compounds suitable for use as raw materials combined with the AI value, based on the standards applied at company (PT. Sinar Tambang Arthalestari, 2023) for portland cement. The AI value is obtained by calculation (1), as follows:

$$AI = \frac{Compound\ SiO_2\ \%}{Compound\ Al_2O_3\%} \quad (1)$$

Then, looking at the different types of minerals can help with the quality data that is already known about claystone. This can help figure out what kind of claystone is the best for Portland cement raw materials based on the minerals that are found in the research area.

The results of the geochemical analysis and types of minerals will later produce information on the quality and types of claystone minerals as raw materials for portland cement in the research area, which are represented in the claystone quality zoning map and tables along with relationship curves for each compound sorted from old-young samples.

4. Analysis Results

The claystone research area is the Halang Formation, which consists of interbedded claystone and sandstone. The determination of deposited environmental facies is based on several parameters, such as lithological characteristics and mineral composition, sediment structure, and grain size variations (Fig. 5). Several parameters were stepwise analysis from facies analysis and facies association to estimate where and how this unit was deposited (A. K. Gibran & Kusworo, 2020; Sun, 2014).

4.1 Stratigraphy of The Research Area

Based on the index map in Fig. 1, This research is carried out in the administrative area of Ajibarang District, Central Java Province. The research area covers six villages, including Tipal Kidur, Karangbawang, Dharmakeradenan, Pancasan, Kracak, and Ajibarang Kulon, and the main watershed (DAS) is the Tajum River. Two of the six villages included in the claystone survey area are Karangbawang and Tipal Kidul Villages.

The Purwokerto-Tegal sheet's regional geological maps (Djuri, 1996) are combined with the existing primary data, it is known that the geology of the research area has four (4) geomorphological units (Brahmantyo & Bandono, 2006), namely the Kracak Syncline Valley Unit, the Tipar Kidul Fault Structure Denudation Plain Unit, the Cilanglung Homocline Ridge Unit, and the Karangbawang Homocline Ridge Unit. The four units are controlled by trellis river flow patterns with subsequent and obsequent river genetics (Fig. 2).

The stratigraphy of old to young layers in the geological survey area (Figs. 4 and 5) is composed of interbedded claystone-sandstone units of the Halang Formation (Tmph), with sedimentary structures such as parallel laminated, wavy laminated, cross laminated, and convoluted structures (Zerlinda & Aditama, 2021). Petrographic analysis shows that this unit contains lithic wacke sandstone and mudstone (Purwasatriya et al., 2021). Next, the Tapak Formation Limestone Unit (Tptl) is dominated by calcarenite limestone (Purwasatriya *et al.*, 2021). Petrographic analysis reveals that there are three types of limestone, namely wackestone, packstone, and grainstone (Rohmana & Achmad, 2019). The next unit is the Interbedded Sandstone-Claystone Unit in the Tapak Formation (Tpt), whose sedimentary structure is parallel lamination (Rohmana & Achmad, 2019). Petrographic analysis shows that this unit contains lithicwacke sandstone and graywacke of claystone (Amin & Susilo, 2019).

Fig. 1 Index Map of Study Area

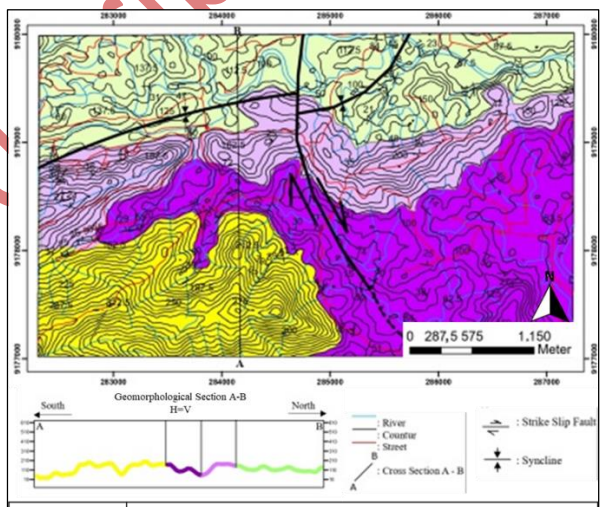

Geomorphological Aspects	Geomorphology Unit			
	Kracak Syncline Valley	Denudational Plain of Dextral Fault	Cibangkung Homocline Ridge	Karangbawang Homocline Ridge
Highest Elevation	137.5 masl.	150 masl.	200 masl.	312 masl.
Lowest Elevation	87.5 masl.	50 masl.	125 masl.	162.5 masl.
Different Heights	50 m	100 m	75 m	150
Slope Percentage	0-2% (flat)	7-15% (slightly steep)	2-7% (sloping)	15-30% (steep)
Drainage Pattern	Trellis	Trellis	Trellis	Trellis
River Valley Shape	U	U	-	V
Lithology	Sandstone and Claystone	Sandstone and Claystone	Limestone	Claystone and Sandstone
Endogenic Process	Fold and Fault	Fault	Uplift, fault	Uplift
Exogenic Process	Erosion, Transportation, Sedimentation, whathering	Erosion, Transportation, Sedimentation, whathering	Erosion, Transportation, Sedimentation, whathering	Erosion, Transportation, Sedimentation, whathering
Geological Structure	Fold and Fault	Fault	Fault	-
Land Use	Settlements, Agriculture	Settlements, Agriculture, Mining	Mining	Settlements, Agriculture

Fig 2. Geomorphological Map of the Research Area

Based on microfossil analysis data, it is known that the age of deposition starts from the Late Miocene to the Pliocene, with inner, middle, and outer neritic depositional environments (Gibran et al., 2022; Isnaniawardhani, 2017). Deposition began in the

interbedded claystone-sandstone unit of the Miocene Halang Formation (Tmph), with a turbidite flow mechanism in a middle neritic environment (Purwasatriya et al., 2021). Furthermore, the Tapak Formation Limestone Unit (Tptl) deposited continuously in the outer neritic environment during the Pliocene. Followed by the deposition of the interbedded sandstone-claystone unit of the Tapak Formation (Tpt) (Astuti et al., 2019). The limestone unit of the Tapak Formation (Tptl) is also present in the deposit. This is possible due to changes in sea level over a certain period of time (Astuti et al., 2017). The structure of the finger is determined based on the area and continuity of this unit and the results of the proportional reconstruction of the lithofacies (Amin & Susilo, 2019; Rizkianto et al., 2023). The deposition of these units was accompanied by volcanic activity, as evidenced by the discovery of primary minerals confirmed by petrographic analysis, such as biotite, plagioclase, and opaque.

At the end of the Pliocene, regional forces triggered tectonic activity (Adhari & Hidayat, 2023; Kurniasih et al., 2023; Safira et al., 2023). At this time, the Kracak syncline fold was formed with a relatively west-east direction, which was deformed in a relatively north-south direction by the Tipar Kidul strike-slip fault.

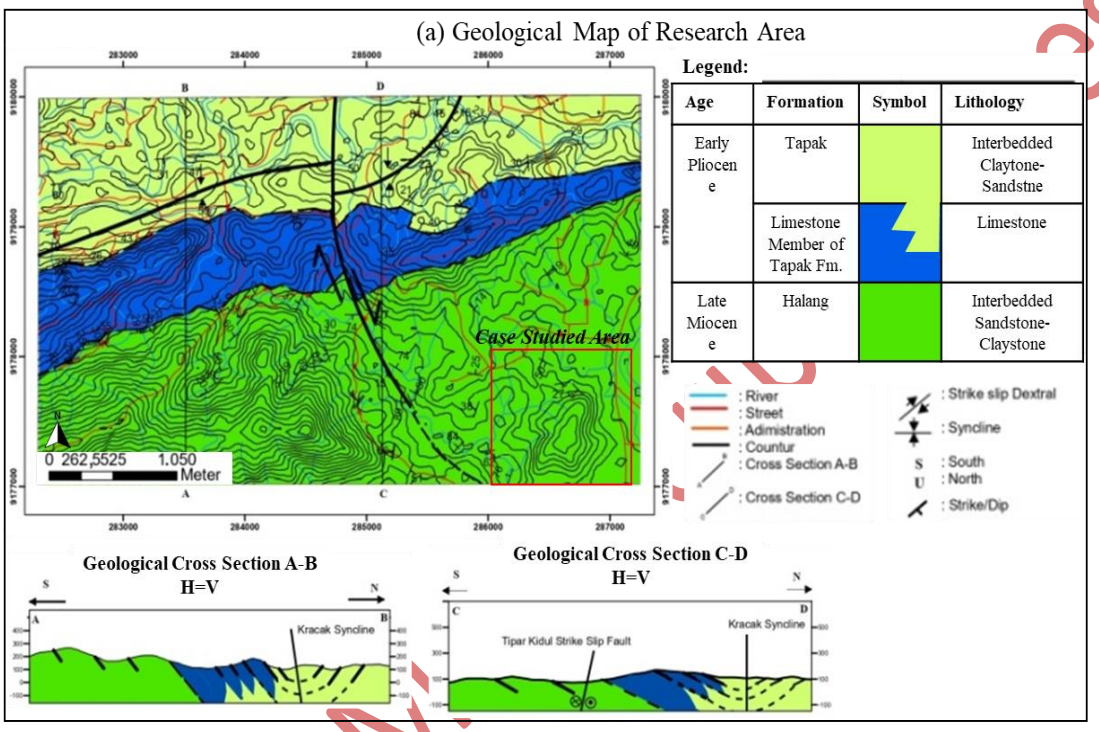

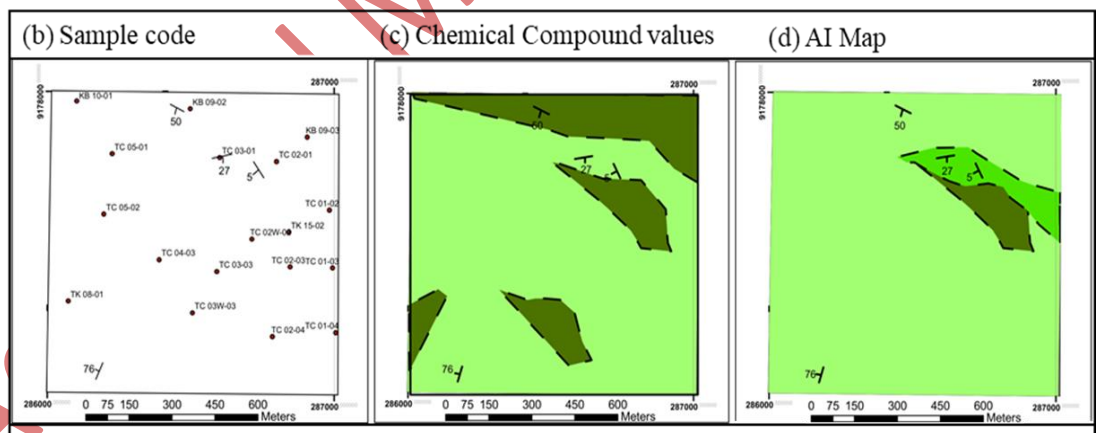

Symbol	PT.Sinar Tambang Arthalestari Laboratory Sample Chemical Compound Values			PT. Sinar Tambang Arthalestari Clasification	Symbol	PT. Sinar Tambang Arthalestari Alumina Index (AI) Value	PT. Sinar Tambang Arthalestari Alumina Index (AI) Classification
	SiO_2 (%)	Al_2C_3 (%)	Fe_2O_3 (%)				
	26,83-50,42	11,18-16,57	3,21-8,53	Not Worth It		4,19%	High
	52-57,75	15,1-19,52	5,78-8,76	Worth It		3,17 - 3,22 %	Good
						2,40 - 3,15 %	Low

Fig. 3. (a) Geological Map of the Research Area; (b) XRF Sample Distribution Map; (c) Claystone Feasibility Quality Map Base on PT. Sinar Tambang Arthalestari Clasification; (d) Clay Quality Map Based on Compound Content Base on PT. Sinar Tambang Arthalestari Clasification

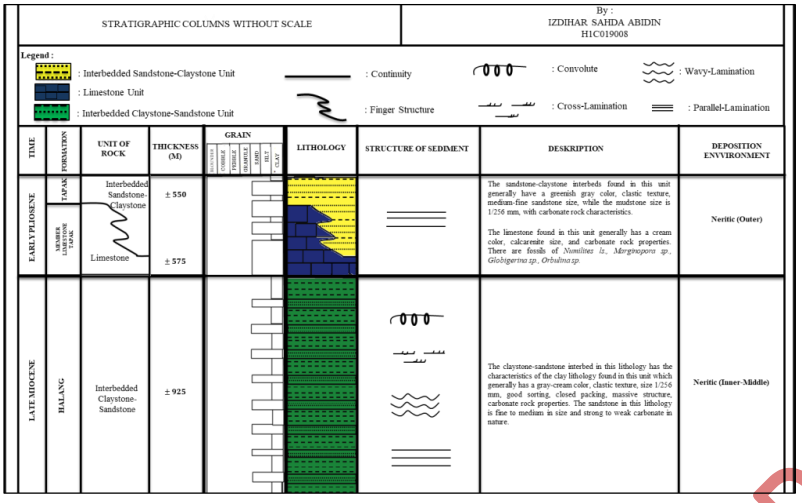

Fig 4. Stratigraphic Columns from the Research Area

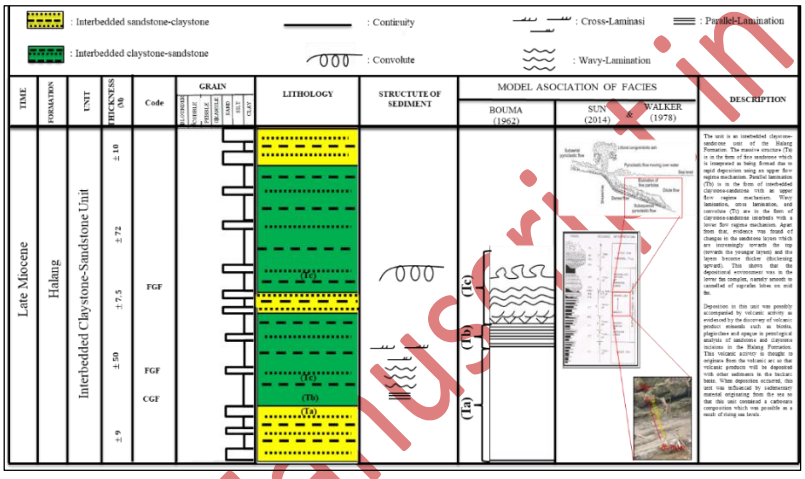

Fig 5 Lithological Profile Of The Turbidite System Of The Claystone Study Area.

Tabel. 1 XRF analysis result

No	Sample Code	Lithology (PT. Sinar Tambang Arthalestari Classification)	SiO_2 (%)	Al_2O_3 (%)	Fe_2O_3 (%)	CaO (%)	MgO (%)	K_2O (%)	Na_2O (%)	SO_3 (%)	AI (Index Alumina)	Index Alumina Classification PT. Sinar Tambang Arthalestari	Geochemical Classification (SiO_2, Al_2O_3, Fe_2O_3) PT. Sinar Tambang Arthalestari
1	KB 10-01	Sandy Carbonate Clay	35,68	14,84	4,61	24,97	2,96	0,41	0,44	0,05	2,40	Low	Not Feasible
2	KB 09-02	Sandy Carbonate Clay	26,83	11,18	3,43	31,47	1,46	0,27	0,35	0,04	2,40	Low	Not Feasible
3	KB 09-03	Clay	40,87	16,57	3,21	22,93	1,82	0,73	0,39	0,06	2,47	Low	Not Feasible
4	TC 05-01	Clay	54,46	19,52	6,95	3,37	2,12	-	-	-	2,79	Low	Feasible
5	TC 03-01	Clay	55,77	17,57	6,6	4,65	2,61	-	-	-	3,17	Good	Feasible
6	TC 02-01	Clay	54,15	18,37	8,47	4,78	3,58	-	-	-	2,95	Low	Feasible
7	TC 05-02	Clay	53,76	18,84	6,48	4,49	2,23	-	-	-	2,85	Low	Feasible
8	TC 01-02	Clay	57,75	17,94	6,85	3,74	2,17	-	-	-	3,22	Good	Feasible
9	TK 15-02	Clay	48,53	11,57	8,53	6,05	2,53	0,42	0,17	0,04	4,19	High	Feasible
10	TC 02W-02	Clay	52,49	18,24	8,48	4,13	3,41	-	-	-	2,88	Low	Feasible
11	TC 04-03	Clay	54,61	19,03	8,76	2,66	3,1	-	-	-	2,87	Low	Feasible
12	TC 02-03	Clay	53,06	18,68	5,78	5,06	1,51	-	-	-	2,84	Low	Feasible
13	TC 01-03	Clay	54,54	20,23	6,68	2,91	2,27	-	-	-	2,70	Low	Feasible
14	TC 03-03	Clay	52	16,61	7,56	8,12	3,7	-	-	-	3,13	Low	Feasible
15	TK 08-01	Clay	42	15,1	4,79	22,72	3,17	0,31	0,09	1,37	2,78	Low	Not Feasible
16	TC 03W-03	Sandy	50,42	16,34	7,88	9,95	4,18	-	-	-	3,09	Low	Not Feasible
17	TC 02-04	Clay	53,54	18,68	8,72	3,06	3,54	-	-	-	2,87	Low	Feasible
18	TC 01-04	Clay	56,85	18,07	7,3	1,86	2,27	-	-	-	3,15	Low	Feasible
Rumus AI (Alumina Indeks) = SiO_2 : $Al2O_3$, Klasifikasi AI Perusahaan : 3.16%-3.44%													

Tabel 2 Geochemical analysis of claystone quality for portland cement.

NO.	SAMPLE CODE	Lithology (PT. Sinar Tambang Arthalestari Classification)	SiO2 (%)	Al2O3 (%)	Fe2O3 (%)	CaO (%)	MgO (%)	K2O (%)	Na2O	SO3	AI (Alumina Index)
			0 35 70	0 12.5 25	0 7.5 15	0 17.5 35	0 2.25 4.5	0 0.4 0.8	0 0.25 0.5	0 0.8 1.6	0 2.25 4.5
1	KB 10-01	Sandy Carbonate Clay									
2	KB 09-02	Sandy Carbonate Clay									
3	KB 09-03	Clay									
4	TC 05-01	Clay									
5	TC 03-01	Clay									
6	TC 02-01	Clay									
7	TC 05-02	Clay									
8	TC 01-02	Clay									
9	TK 15-02	Clay									
10	TC 02W-02	Clay									
11	TC 04-03	Clay									
12	TC 02-03	Clay									
13	TC 01-03	Clay									
14	TC 03-03	Clay									
15	TK 08-01	Clay									
16	TC 03W-03	Sandy									
17	TC 02-04	Clay									
18	TC 01-04	Clay									
SiO2, Al2O3, Fe2O3 and AI of PT. Sinar Tambang Arthalestari Classification: SiO2 : Min. 52% Al2O3 : Max. 25% Fe2O3 : Max. 15% AI : 3.16-3.44 %			Low High	Normal High	Normal High						Low High

6. Discussion

6.1 Lithological Profile Of The Turbidite System Of The Claystone Study Area.

Based on Fig. 4, this unit is an Interbedded Claystone-Sandstone Unit of the Halang Formation. In units based on (Bouma, 1964) there are several appearances of turbidite current structures. First, the massive gradded bedding structure (Ta) is in the form of fine sandstone and is thought to have formed through rapid deposition using a turbidity mechanism. Parallel stacking (Tb) is interbedded claystone-sandstone with an upper flow regime mechanism. Wavy lamination, cross lamination, and convolute (Tc) are interlayer layers of mudstone and sandstone with lower flow regime mechanisms. Furthermore, we found evidence that the sandstone layers shifted upwards, towards younger layers, and thickened up. This shows that the depositional environment is a subaqueous complex (Walker, 1992), namely channeling from the fine lobe at the top of the fan to the mid fan (Sun, 2014).

The deposition of this unit may be related to volcanic activity, which is indicated by the discovery of volcanic minerals such as biotite, plagioclase, and opaque in petrographic analysis of the sandstone and claystone incisions of the Halang Formation. We believe that this volcanic activity takes place in volcanic arcs, depositing volcanic products in the back arc basin alongside other sediments. At the time of deposition, this unit was influenced by sedimentary material originating from the sea so that it had a carbonate composition, which was made possible by rising sea levels.

6.2 XRF Graph of Clay-Sandy Clay-Sandy Samples in a Clay Mine.

The results of the XRF analysis of 18 samples (Table 1) are sorted from oldest (No. 18) to youngest (No. 1) and show that the compound values experienced several changes over time. We analyzed these changes using curves based on compound content and alumina index. Element change rate curves are shown in Table 2.

Based on table 1, samples with codes TC 01-04, TC 02-04, TC 03W-03, and TK 08-01 generally have smaller SiO_2, Al_2O_3, and Fe_2O_3 compound values. SiO_2 values are 56.86%–42%, Al_2O_3 is 18.68%–15.10%, and Fe_2O_3 is 18.72%–4.79%. Meanwhile, the overall value of CaO compounds increased by 1.86% to 22.72%. For the MgO compound, the value increases in the range of 2.27% to 4.18%. Even though there was an overall increase in value, the MgO compound in the sample coded TK 08-01 experienced a decrease in MgO value of 3.17%. Based on the qualifications for SiO_2, Al_2O_3, and Fe_2O_3 content based on the raw material standards applicable at PT. Sinar Tambang Arthalestari, two of the four samples, namely samples TC 01-04 and TC 02-04, are still classified as suitable for use as cement raw materials. This is because the values of SiO_2, Al_2O_3, and Fe_2O_3 are still within the normal limits of applicable raw materials. AI calculations were carried out to determine the ideal rock quality level for use as raw material for cement, and it was found that three claystone samples and one sandstone sample had AI quality values in the range of 2.78%–3.15%. Therefore, these rocks were assessed as below standard normal and less than ideal for use as raw materials for cement.

Samples coded TC 03-03, TC 01-03, TC 02-03, TC 04-03, TC 02W-02, and TK 15-02 generally have stable SiO_2 and Al_2O_3 values. SiO_2 is relatively in the range of 52%–54.61%, and Al_2O_3 is 16.61%–20.23%. In general, the values were stable; however, for the SiO_2 and Al_2O_3 compounds in sample TK 15-02, the values decreased for SiO_2 by 48.53% and Al_2O_3 by 11.57%. Fe_2O_3 values

decreased, ranging from 7.56% to 5.78% for samples TC 03-03, TC 01-03, and TC 02-03, and increased and stabilized for samples TC 04-03 and TC 02W-02. TK 15-02, the value has been recorded, and the range is 8.48% to 8.76%. Meanwhile, the value of CaO compounds experienced an overall decrease in the range of 8.12% to 2.66%. The MgO compound decreased in value, with values ranging from 3.70% to 1.51%. Even though the value decreased, the MgO compound increased in samples coded TC 04-03 and TC 02W-02 with MgO values between 3.1% and 3. 41%, and the MgO value again decreased from 3.1% to 3.41% in the sample coded TK 15-02. Verify the qualifications for SiO_2, Al_2O_3, and Fe_2O_3 content based on the raw material standards applicable at PT. Sinar Tambang Arthalestari. Of the six samples, namely sample TK 15-02, only one was found to be unfit to be used as raw material. Because the Al_2O_3 value is below normal standards. When carrying out AI calculations to determine the quality level of rock used as raw material for cement, it was found that six mudstone samples had two AI quality values. First, AI with a value of 3.13% to 2.70% is below the normal standard for cement raw materials, and AI with a value of 4.19% is above the normal standard or exceeds the normal AI. Therefore, it is also less than ideal for use as a raw material for cement, according to current standards.

Samples coded TC 01-02, TC 05-02, TC 02-01, TC 03-01, and TC 05-01 have relatively stable SiO_2 and Al_2O_3 compound values, with the SiO_2 value range being 53.76% to 57.75%, and Al_2O_3 to 17.57%-19.52%. Although Fe_2O_3 values tend to be relatively stable in the range of 6.48% to 6.95%, sample TC02-01 recorded a significant increase in Fe_2O_3 values, 8.47%. The value of CaO compounds is generally stable and relatively low, ranging from 3.37% to 4.78%. The MgO compounds' value increased from 2.17% to 3.58%. Even though the value increased, the MgO compound in samples coded TC 03-01 and TC 05-01 decreased, with MgO values ranging from 2.61% to 2.12%. Verify the qualifications for SiO_2, Al_2O_3 and Fe_2O_3 content based on the raw material standards applicable at PT. Sinar Tambang Arthalestari. Five samples are suitable for use as raw materials. When carrying out AI calculations to determine the ideal level of rock quality used as raw material for cement, it was found that five mudstone samples had two AI quality values. First, AI in the range of 2.79% to 2.95% is found in rocks with quality below normal quality standards and is less than ideal for use as a raw material for cement. Apart from that, the AI value is between 3.22 - 3.17% including good quality certification or being at the ideal AI standard for cement raw materials. Good quality AI is coded TC 01-02 and TC 03-01 (Table 2).

Samples coded KB 09-03 and KB 09-02 have SiO_2 and Al_2O_3 compound values, with SiO_2 values ranging from 40.87% to 26.83% and Al_2O_3 values decreasing gradually from 16.57% to 11.18%. In the KB 10-01 sample, the values of SiO_2 and Al_2O_3 compounds increased slightly. So for this sample, the SiO_2 value is 35.68 and the Al_2O_3 value is 14.84%. Meanwhile, the Fe_2O_3 compound in the three samples gradually increased from around 3.21% to 4.61%. An increase in the Fe_2O_3 value indicates more extensive oxidation. Then, the value of the CaO compound generally increased in the range of 22.93% to 31.47% for samples KB 09-03 and KB 09-02 and decreased with a percentage value of 24.97% for CaO in sample KB 10-01. For MgO compounds, the values for samples KB 09-03 and KB 09-02 decreased in the range of 1.82% to 1.46%. In the KB 10-01 sample, the MgO value increased to 2.96%. Verify the qualifications for SiO_2, Al_2O_3, and Fe_2O_3 content based on the raw material standards applicable at PT. Sinar Tambang Arthalestari, which are not suitable for use as raw material. When we carried out AI calculations to determine the quality level of the rocks used for making cement, the AI quality values obtained for sample 1 of claystone and sample 2 of sandy clay were 2.47%–3.40%. Therefore, this rock is considered to have a quality below normal standards and is less than ideal for use as a raw material for cement.

6.3 Clay Mineral Types

Based on Fig. 6, the TK 1 sample code in the claystone research area is located at the bottom. Macroscopically, outcrops tend to be relatively west-east oriented, with light-dark gray claystone lithology, clastic texture, size 1/256 mm, well sorted, closed packing, massive structure, and carbonate. Based on the results of SEM analysis at a magnification of 30 µm, it is known that the TK 1 sample is mostly composed of illite and calcite minerals (Worden & Morad, 2003). The results of this analysis are identified based on mineral morphology. The mineral illite can be recognized by its ribbon-like, fibrous or elongated mineral shape. The calcite mineral has a rhombic morphology.

Based on Fig. 7, the results of digestion and SEM were recorded using sample code TK 2 in the central part of the claystone research area. Macroscopically, the sample outcrop has a relative northwest-southeast orientation, brownish gray claystone lithology, clastic texture, size 1/256 mm, very well sorted, dense filling, and massive. Has the structural characteristics and properties of carbonate rocks. Based on the results of SEM analysis at a magnification of 20 µm, it is known that the TK 2 sample is mostly composed of smectite and quartz minerals. The results of this analysis are identified based on mineral morphology. The smectite mineral can be recognized by its mineral shape which looks irregular and has a characteristic structure, namely "honeycomb", (Theng, 2019). The quartz mineral in the sample has elongated and angular (Itamiya, 2019).

Based on Fig. 8, is an outcrop and SEM results with sample code KB 1 taken in the top of the claystone study area. Megascopically, the sample outcrop has a relatively southwest-northeast direction. This outcrop has the characteristic lithology of light gray-brown claystone. The texture is included in the classic texture. The grain size is at a value of 1/256 mm. The existing sorting is included in the good sorting type. The packaging is a type of closed packaging. It has a massive

structure, and the nature of the rock is carbonate. Meanwhile, based on the results of SEM analysis with a magnification of 20µm, it is known that this sample is dominated by calcite and quartz minerals. The results of this analysis are identified based on the morphology of the mineral. Where the mineral calcite has a rhombic morphology (Worden & Morad, 2003). Meanwhile, the mineral quartz has an angular grain morphology (Itamiya, 2019).

The composition and quality of the claystone in the claystone research area were measured based on the results of chemical compound analysis using the XRF analysis method and morphological analysis of the claystone minerals using the SEM analysis method. Then, we randomly selected eighteen (18) samples for the chemical compound analysis. As for the quality of the samples based on compound content, thirteen (13) samples were declared suitable because they met the normal standards for compounds that may be used as raw materials based on company classification, with a range of SiO_2 of 52%–57.75%, Al_2O_3 of 15.1%–19.5%, and Fe_2O_3 of 5.78%–8.76%. Based on the AI value, there are two (2) samples that have the ideal value to be used as cement raw materials, with a range of 3.17%–3.22% according to the company's AI raw material standards. Mineral composition based on the morphological analysis of minerals taken from three (3) random samples of claystone, it is known that in the area below the plot, illite and calcite minerals were found with SiO_2 and Al_2O_3 values that generally decreased. In the middle area of the plot, smectite and quartz minerals with SiO_2 and Al_2O_3 values tend to be stable. In the upper area of the plot, calcite and quartz were found with SiO_2 and Al_2O_3 values that gradually decreased. The presence of the mineral smectite indicates that its properties are crucial for the formation of clinker. The smectite mineral in question has good temperature stability and ion exchange properties. Based on a literature study conducted on the chemical feasibility of clay minerals as a raw material for Portland cement in Tritih Lor Village, Jeruklegi District, Cilacap Regency (Wijaya, 2005) which revealed that this mineral has the most appropriate composition of chemical elements in the clinker formation reaction. From the analysis results, it was found that almost 75% of the claystone study area (Fig.3.c) is an area that is suitable to be taken as raw material for cement coupled with the discovery of ideal areas for cement raw materials by 20% (Fig.3.d) based on the PT. Sinar Tambang Arthalestari.

This study looks at the connection between rock layers and geochemical data in the area. It is known that as rocks get younger, their SiO_2 and Al_2O_3 compound contents go down, while their CaO and MgO compound contents go up. This can be understood because the younger the rock, the lithology has a fairly high carbonate sand content. The high carbonate sand content is possible due to the influence of sedimentary material originating from the sea, which has a carbonate composition caused by rising sea levels.

Based on the description that has been explained based on stratigraphic, geochemical, and mineral type data in the claystone research area, the decision to make this area a claystone mine for cement raw materials based on geological conditions is correct.

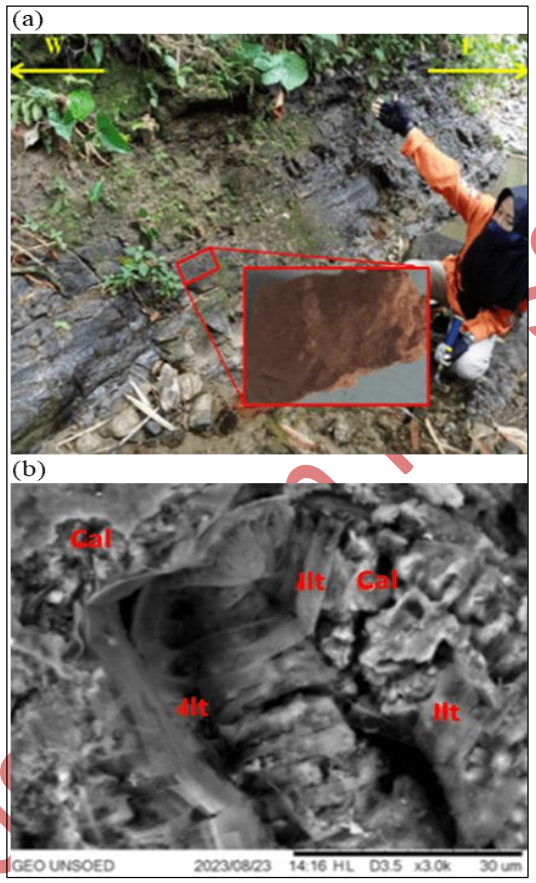

Fig.. 6. (a) Outcrop of TK 1 sample; (b) SEM results of TK 1 samples (Ilt: Illite; Cal: Calcite)

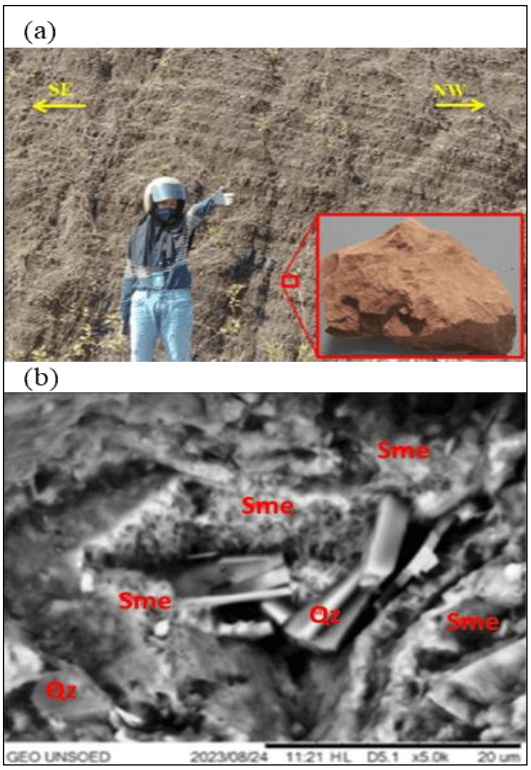

Fig. 7 (a) Outcrop of TK 2 Sample; (b) SEM results of TK 2 samples (Sme: Smectite; Qz: Quartz)

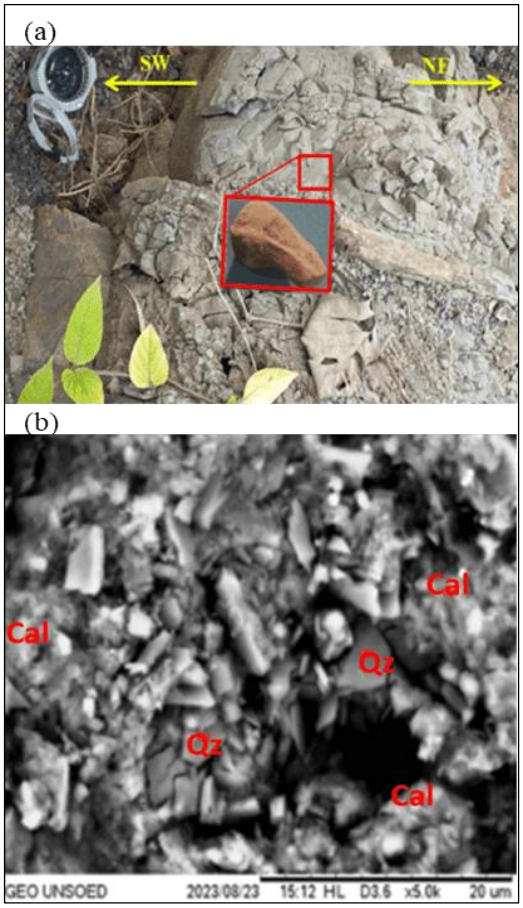

Fig. 8 (a) Outcrop of KB 1 sample; (b) SEM results of KB 1 samples (Cal:Calcite; Qz: Quartz)

7. Conclusion

The relationship between stratigraphy and geochemical data in the research area that the younger the rock, the compound content in general has a decreasing value of SiO_2 and Al_2O_3, while the value of CaO and MgO compounds has increased. Because the younger the rock, the lithology with a fairly high carbonate sand content. The high carbonate sand content is possible due to the influence of sedimentary material originating from the sea so that it has a carbonate composition caused by rising sea levels. Therefore, the quality of claystone towards younger ages becomes worse for use as raw material for Portland cement. There are 13 of 18 samples that are suitable as research locations because they meet the general criteria for compounds that can be used as raw materials based on company classification with a range of SiO_2 52%-57.75%, Al_2O_3 15.1%-19.52%, Fe_2O_3 5.78% - 8.76%.

Mineral composition is based on morphological analysis of minerals collected from three random claystone samples. The minerals illite and calcite were found in the area below the area, and SiO_2 and Al_2O_3 values were found to decrease overall. In the central region of the area, smectite and quartz minerals tend to be stable at SiO_2 and Al_2O_3 values. At the top of the plot, calcite and quartz were found with decreasing SiO_2 and Al_2O_3 values. The analysis results show that almost 75% of the claystone research area (Fig. 6.) is suitable for use as raw material for cement reinforced with the presence of smectite minerals, and there are two samples with ideal AI values (3.16% to 3.22%) based on company. This research has a positive influence in terms of characterizing limestone as a raw material for cement through the utilization of geochemical analysis and electron microscopy to get further insights into the evaluation of limestone quality.

Acknowledgments

The author thanks to PT. Sinar Tambang Arthalestari for providing the opportunity to facilitate the author when collecting data and laboratory analysis for XRF analysis. The author would like to thank the supervisor and the entire academic community of the Department of Geological Engineering, Jenderal Soedirman University, who have provided convenience in supporting the realization of this article, including laboratory analysis for SEM analysis.

References

Adhari, M. R., & Hidayat, R. (2023). A geological overview of the limestone members of the Woyla Group of Sumatra, Indonesia. *Journal of Geoscience, Engineering, Environment, and Technology*, *8*(3), 189–195. https://doi.org/10.25299/jgeet.2023.8.3.12190

Amin, M. H. A., & Susilo, B. K. (2019). Lingkungan pengendapan Formasi Tapak daerah Samudra, Kabupaten Banyumas, Jawa Tengah. *Proceeding of Innovation of Engineering and Science Research*, 252–259.

Astuti, B. S., Isnaniawardhani, V., Abdurrokhim, & Sudradjat, A. (2017). *Micro Tectonic At North Serayu Basin, Central Java: Case Study At Type Locality of Rambatan Formation*. 233–237.

Astuti, B. S., Isnaniawardhani, V., Abdurrokhim, & Sudradjat, A. (2019). Sedimentation Process of Rambatan Formation in Larangan Brebes, North Serayu Range, Central Java. *Indonesian Journal on Geoscience*, *6*(2), 141–151. https://doi.org/10.17014/ijog.6.2.141-151

Bouma, A. H. (1964). *Developments In Sedimentology Turbidites*.

Brahmantyo, B., & Bandono. (2006). Klasifikasi Bentuk Muka Bumi (Landform) untuk Pemetaan Geomorfologi pada Skala 1:25.000 dan Aplikasinya untuk Penataan Ruang. *Jurnal Geoaplika*, *1*(2), 071–078.

Djuri, M. (1996). *Peta Geologi Regional Lembar Purwokerto-Tegal, skala 1:100.000*.

Gibran, A. K., & Kusworo, A. (2020). Fasies dan Lingkungan Pengendapan Formasi Kanikeh , Cekungan Bula, Maluku. *RISET Geologi Dan Pertambangan*, *30*(2), 171–186. https://doi.org/10.14203/risetgeotam2020.v30.1108

Gibran, A. K., Kusworo, A., Wahyudiono, J., Sunan, H. L., Aeni, D. N., & Alghazali, A. (2020). Reservoir Characteristic of Triassic Sandstone, Eastern Seram, Maluku, Indonesia. *IOP Conference Series: Materials Science and Engineering*, *982*(1). https://doi.org/10.1088/1757-899X/982/1/012045

Gibran, A. K., Setijadi, R., Purwasatriya, E. B., Ananda, D. R., & Nabil, M. I. (2022). Biostratigrafi Dan Sedimentologi Plio-Pleistosen Daerah Bumiayu - Tonjong, Jawa Tengah. *Jurnal Geologi Kelautan*, *20*(1), 33–44. https://doi.org/10.32693/JGK.20.1.2022.738

Gibran, A., Kusworo, A., Wahyudiono, J., & Purwasatriya, E. (2022). Proses Diagenesis Batupasir Formasi Kanikeh, Seram Bagian Timur, Maluku, IndonesiaSandstone Diagenesis Process of Kanikeh Formation, Eastern Seram, Molucca, Indonesia. *Journal of Geology and Mineral Resources*, *23*(200), 113–122.

Gifford, J. N., Platt, B. F., Yarbrough, L. D., O'reilly, A. M., & Al Harthy, M. (2020). Integrating petrography, x-ray fluorescence, and u-pb detrital zircon geochronology to interpret provenance of the mississippian hartselle sandstone, USA. *Journal of Geology*, *128*(4), 337–370. https://doi.org/10.1086/709700

Goldstein, J. I., Newbury, D. E., Michael, J. R., Ritchie, N. W. M., Henry, J., Scott, J., & Joy, D. C. (2018). *Scanning Electron Microscopy and X-Ray Microanalysis*.

Grabau, A. W. (1904). *On The Classification Of Sedimentary Rocks*. American geologist.

Isnaniawardhani, V. (2017). *Prinsip dan Aplikasi Biostratigrafi*.

Itamiya, H. (2019). Analysis of the surface microtextures and morphologies of beach quartz grains in Japan and implications for provenance research. *Progress in Earth and Planetary Science*, *6*(1). https://doi.org/10.1186/s40645-019-0287-9

Kurniasih, A., Adha, I., Dalimunthe, H. L., Setyawan, R., Khorniawan, W. B., Qadaryati, N., Jayanti, A. G. R., & Wijaya, F. P. (2023). Biostratigraphic Interpretation of Lutut Beds, Kerek Formation, Based on Foraminifera Fossils. *Journal of Geoscience, Engineering, Environment, and Technology*, *8*(2), 105–111. https://doi.org/10.25299/jgeet.2023.8.2.12462

Marin, J., Winarno, T., & Fairuz, S. N. (2022). Characteristics of Kedondong Trass and Bobos Trass as Cement Raw Material, Cirebon, West Java, Indonesia. *Journal of Geoscience, Engineering, Environment, and Technology*, *7*(1), 27–33. https://doi.org/10.25299/jgeet.2022.7.1.8180

Pettijohn, F. J. (1975). *Sedimentary Rock Third Edition*. Harper & Row.

PT. Sinar Tambang Arthalestari. (2023). *Database Hasil Survey*.

Purwasatriya, E. B., Gibran, A. K., Aditama, M. R., & Waluyu, G. (2021). Sedimentologi dan Tektonostratigrafi Formasi Halang di Cekungan Banyumas serta Potensinya untuk Reservoir Hidrokarbon. *Jurnal Geologi Dan Sumberdaya Mineral*, *22*(3), 153–163. https://doi.org/10.33332/JGSM.GEOLOGI.V22I3.640

Rizkianto, Y., Choiriah, S. U., Subandrio, A., Haty, I. P., Isnani, D. K., Nurwantari, N. A., Syah Darmawa, M. A., & Wirandoko, H. (2023). Trace Fossils Of The Selorejo Formation, Rembang Zone, North East Java Basin, Indonesia. *Journal of Geoscience, Engineering, Environment, and Technology*, *8*(3), 183–188. https://doi.org/10.25299/jgeet.2023.8.3.10454

Rohmana, R. C., & Achmad, A. (2019). Analisis Sedimentologi dan Stratigrafi untuk Rekonstruksi Model Lingkungan Pengendapan : Mengungkap Proses Pembentukan Formasi Tapak , Abstrak Objek studi difokuskan pada Formasi Tapak yang terendapkan pada Miosen Akhir – Pliosen Akhir di Sub-Cekungan Ban. *Geoscience Dan Teknologi*, *2* no.*3*(58), 126–134.

Safira, F., Purwasatriya, E. B., & Gibran, A. K. (2023). Early to Middle Miocene Dissectec Arc of Karangsambung Area: A Case Study of Waturanda and Penosogan Formations Provenance. *Journal of Earth and Marine Technology (JEMT)*, *3*(2), 124–140. https://doi.org/10.31284/j.jemt.2023.v3i2.4535

Sun, M. (2014). *What's The Difference Between Subaerial And Subaqueous Originated Subaqueous Pyroclastic Rocks*. Chinese Academy of Sciences.

Theng, B. K. (2019). *Clay Mineral Catalysis of Organic Reactions*.

Walker, R. G. (1992). *Facies Models And Modern Stratigaphic Concepts*.

Welton, J. E. (2020). SEM Petrology Atlas. In *SEM Petrology Atlas* (Issue 4). https://doi.org/10.1306/mth4442

Wijaya. (2005). *Kelayakan Kimia Mineral Lempung sebagai Bahan Baku Semen Portland di Desa Tritih Lor, Kecamatan Jeruklegi, Kabupaten Cilacap : Studi Kasus Pengembangan Eksplorasi Mineral Lempung sebagai Bahan Baku Semen di PT. Semen Cibinong Tbk (Persero) Pabrik Cilacap*. Gadjah Mada Yogyakarta.

Wilkins, A. D. (2014). Terminology and the classification of fine grained sedimentary rocks – is there a difference between a claystone, a mudstone and a shale? *Geology*, *1950*, 1–12.

Worden, R. H., & Morad, S. (2003). *Clay mineral cements in sandstones*. Blackwell Pub.

Zerlinda, D. R., & Aditama, M. R. (2021). Interpretasi Geologi Daerah Cidora Dan Sekitarnya, Kecamatan Lumbir, Kabupaten Banyumas, Jawa Tengah. *Jurnal Pendidikan Dan Teknologi Indonesia*, *1*(2). https://doi.org/10.52436/1.jpti.11